AMERICAN SOCIETY FOR MICROBIOLOGY | Journal of Bacteriology®

RESEARCH ARTICLE

Cooperativity in ATP Hydrolysis by MopR Is Modulated by Its Signal Reception Domain and by Its Protein and Phenol Concentrations

Jayanti Singh,[a] Ruchi Anand,[a] Amnon Horovitz[b]

[a]Department of Chemistry, Indian Institute of Technology Bombay, Mumbai, Maharashtra, India
[b]Department of Chemical and Structural Biology, Weizmann Institute of Science, Rehovot, Israel

ABSTRACT The NtrC family of AAA+ proteins are bacterial transcriptional regulators that control σ54-dependent RNA polymerase transcription under certain stressful conditions. MopR, which is a member of this family, is responsive to phenol and stimulates its degradation. Biochemical studies to understand the role of ATP and phenol in oligomerization and allosteric regulation, which are described here, show that MopR undergoes concentration-dependent oligomerization in which dimers assemble into functional hexamers. The oligomerization occurs in a nucleation-dependent manner with a tetrameric intermediate. Additionally, phenol binding is shown to be responsible for shifting MopR's equilibrium from a repressed state (high affinity toward ATP) to a functionally active, derepressed state with low-affinity for ATP. Based on these findings, we propose a model for allosteric regulation of MopR.

IMPORTANCE The NtrC family of bacterial transcriptional regulators are enzymes with a modular architecture that harbor a signal sensing domain followed by a AAA+ domain. MopR, a NtrC family member, responds to phenol and activates phenol adaptation pathways that are transcribed by σ54-dependent RNA polymerases. Our results show that for efficient ATP hydrolysis, MopR assembles as functional hexamers and that this activity of MopR is regulated by its effector (phenol), ATP, and protein concentration. Our findings, and the kinetic methods we employ, should be useful in dissecting the allosteric mechanisms of other AAA+ proteins, in general, and NtrC family members in particular.

KEYWORDS AAA+, allostery, oligomerization, phosphate-binding protein, phenol

The AAA+ (ATPases Associated with various cellular Activities) superfamily of proteins are ubiquitous and involved in numerous and diverse biological processes such as cell cycling, protein folding and degradation, disassembly of macromolecular complexes, and membrane fusion (1, 2). AAA+ are ATP-fuelled molecular machines that are often found to exist as ring complexes (3, 4). ATP binding and hydrolysis take place in their conserved nucleotide binding domain (NBD) (2) and lead to conformational changes that can generate mechanical force essential for their function (5, 6). Most AAA+ proteins form assemblies of two or more subunits to perform their function (7). The heterogeneity in the function of this family of proteins is mostly due to their specific accessory domains and oligomeric structures (8). Such differences impact the AAA+'s kinetics of nucleotide binding and hydrolysis, stability, and the mechanisms by which conformational changes are coupled to their function (8, 9). Despite much previous research on members of AAA+, the relationships between their structures and functions are still not well understood. Some attempts to understand allosteric regulation in these multi-subunit proteins have been done using the well-established Monod–Wyman–Changeux (MWC) and the Koshland–Némethy–Filmer (KNF) models of protein cooperativity (10, 11).

Editor Patricia A. Champion, University of Notre Dame

Address correspondence to Amnon Horovitz, Amnon.Horovitz@weizmann.ac.il, or Ruchi Anand, ruchi@chem.iitb.ac.in.

The authors declare no conflict of interest.

Received 7 June 2022
Accepted 20 June 2022

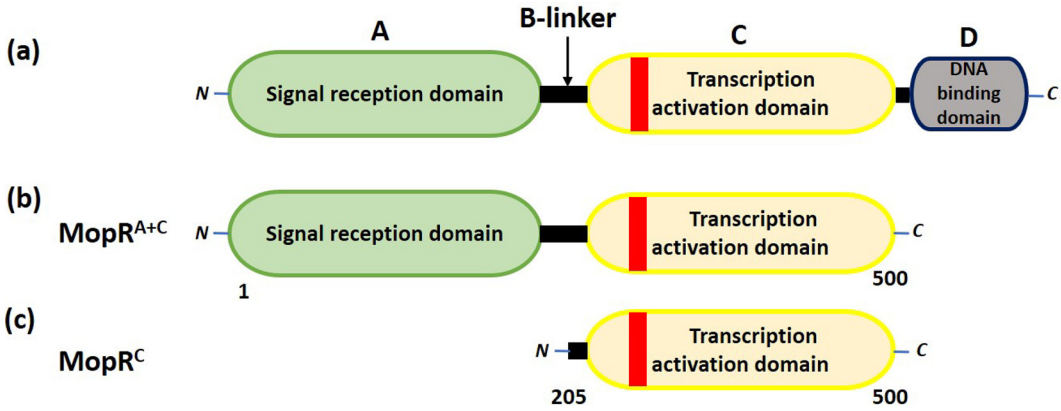

FIG 1 Domain organization. The domain organization of (a) the NtrC family proteins and the truncated constructs of MopR designated (b) $MopR^{A+C}$ and (c) $MopR^{C}$ (ATP binding site is shown in red).

Members of the NtrC family of AAA+ proteins aid in converting the inactive closed σ54-dependent RNA polymerase (RNAP) promoter complex to an open active state; thereby effecting transcription of genes involved in selected downstream pathways (12). These proteins belong to the broader family of bacterial enhancer binding proteins that are known to assist in onset of bacterial virulence and also promote survival under stressful conditions by triggering specific pathways that help cope with the external stimuli (12). NtrC family regulators are characterized by modular domain organization with a unique variable signal reception domain (A) connected via a short so-called B-linker to a highly conserved ATPase domain (C) and a C-terminally located DNA binding domain (D) (Fig. 1a) (13, 14). The C-terminal DNA binding domain forms a helix-turn helix motif and binds to an activation site which is generally ~200 bp upstream of the transcription regulation site where the NtrC-σ54-RNAP complex assembles (12). The central conserved ATPase domain is composed of the seven conserved segments, common to AAA+ superfamily members, with two additional β-hairpin insertions that form the two loops close to the central pore (12, 14). The loops are believed to be important for effecting the mechano-function of the enzyme via interaction with the σ54-RNAP complex (15, 16). The N-terminal signal reception domain is the one that senses the external stimuli and makes the protein responsive to environmental cues (12). The signal can be transferred to the enzyme via either phosphorylation, binding of a specific ligand, or protein-protein interactions (12). The founding members of the NtrC family, NtrC, NtrC1, and NtrC4, have relatively smaller signal reception domains, and the primary mode of signal transduction in these proteins is by phosphorylation of a specific aspartate residue (17–19). In contrast, the MopR family subgroup members have relatively medium-sized signal sensing domains that span around 200 residues (20). These members sense different xenobiotics as exemplified by the response of XylR to benzene, DmpR to 2, 3-dimethylphenol, and MopR and PoxR to phenol (20, 21).

Based on the previous structural studies of the NtrC members, it has been proposed that these proteins exist as dimers, which undergo effector-promoted assembly into higher-order oligomers in which the interfaces serve as the ATP binding and hydrolysis sites (22). The active oligomeric state is not well documented for these NtrC superfamily systems. For the proteins belonging to the MopR subclass, such as MopR and its close homolog PoxR, the crystal structures of their signal reception domains were solved as dimers (20, 21). The crystal structure of DmpR, which belongs to the same subclass, shows that although the signal reception domain has a similar dimeric assembly like that of MopR and PoxR, the overall structure in the presence of the AAA+ ATPase domain is a tetramer (23). The truncated construct of NtrC1 that contains only the AAA+ ATPase domain and lacks the signal reception domain has been solved as a heptameric assembly (17). In the case of the full-length inactivated form like that

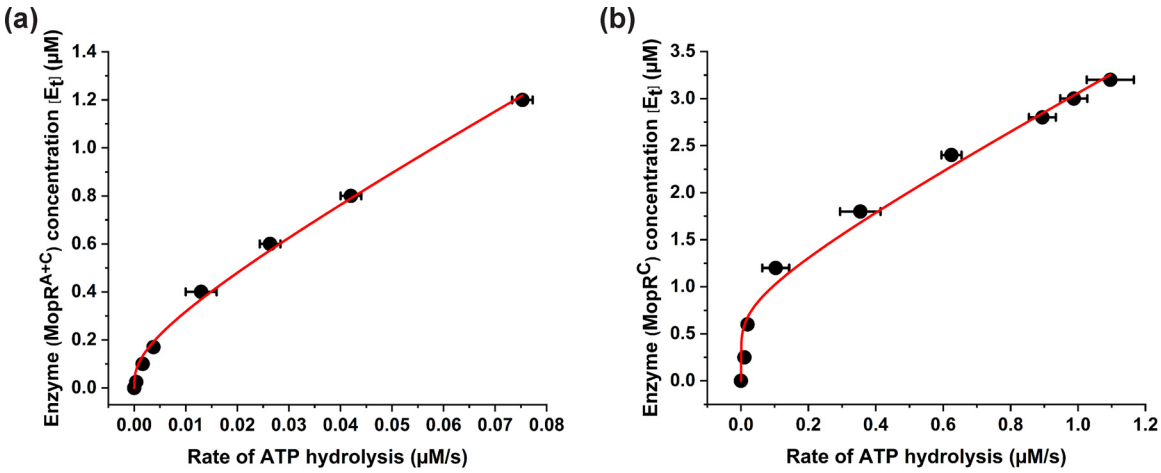

FIG 2 Protein concentration dependence of ATPase activity. Plots of enzyme concentration ([E_t]) versus rate of ATP hydrolysis for (a) MopR^{A+C} and (b) MopR^{C}.

solved for NtrX, however, a dimer was the predominant form captured (24). Although structural snapshots of a subset of the members are available, an understanding of the origins of the heterogeneity in the oligomerization states of these proteins and the factors regulating their assembly and activation is still lacking. Moreover, the modes of inter- and intra-domain allostery in this family of regulators are also still not well-understood, in part, because of the plethora of possible effects due to effector and nucleotide binding. Thus, a question that arises from the review of the current literature on these systems is whether the functional forms of MopR subgroup members, like other AAA+ members, are higher-order structures such as hexamers or heptamers or are the dimeric or tetrameric units capable to elicit function.

Here, in an effort to unveil the allosteric regulation in MopR, and to establish its functional oligomeric state, we carried out a kinetic analysis in which the concentrations of protein, ATP, and phenol were varied. The results provide insights into the mode by which MopR achieves its functional state. Furthermore, this study also highlights the evolutionary relationship of the MopR system with other members of AAA+ superfamily and suggests that some crucial underlying structural similarities can have a widespread impact on the mechanistic properties of these proteins. Our results indicate that characteristic secondary structure insertions might be responsible for the distinctive oligomerization profile and subsequent functional activation of this system.

RESULTS

Constructs of MopR were generated that comprise the central NBD-containing transcription activation domain, MopR^{C} (Fig. 1c) and the transcription activation domain fused via the B-linker to the C-terminus of the N-terminally located signal reception domain, MopR^{A+C} (Fig. 1b).

Initial rates of ATP hydrolysis by MopR^{A+C} and MopR^{C} were measured as a function of their monomer concentration at a saturating concentration of ATP (7 mM), in the absence of phenol. The data were found to be nonlinear (Fig. 2) for both MopR^{A+C} and MopR^{C}, thereby indicating that these proteins are in equilibrium between various oligomeric states that differ in their ATPase activities. The data were, therefore, fitted to Equation 5 derived by assuming that there exists an equilibrium between an inactive monomeric (or dimeric) species and the active hexameric species. The data fitted best to a dimer-hexamer equilibrium in the case of MopR^{A+C} and a monomer-hexamer equilibrium in the case of MopR^{C}. The data fitting also provided estimates of the values of the catalytic rate constant (k_{cat}) of the hexamer and equilibrium constant (K_{eq}) of hexamerization. The k_{cat} and K_{eq} values for MopR^{A+C} were found to be 0.09 $\pm$ 0.01 s^{-1}

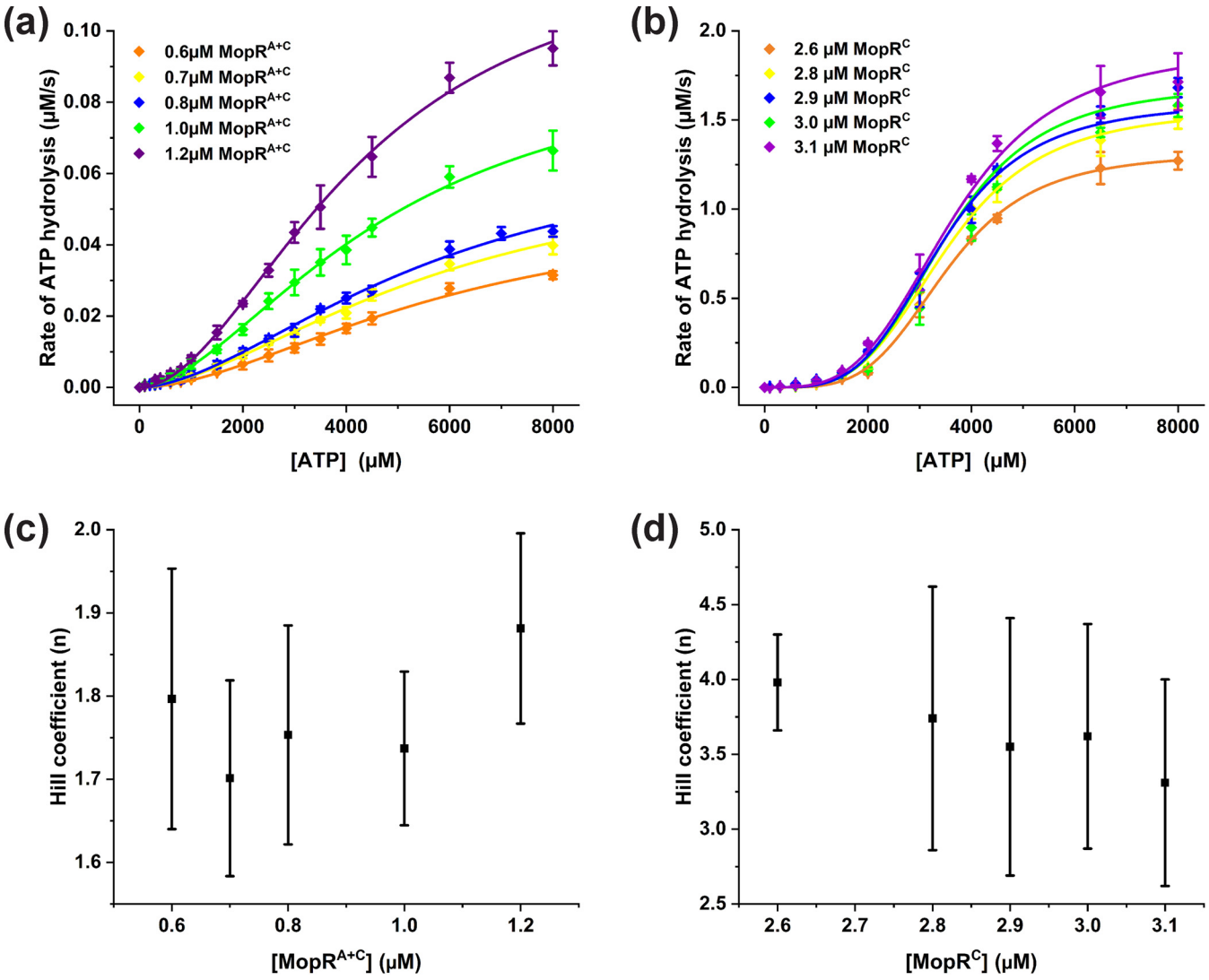

FIG 3 Effect of protein concentration on allosteric properties. Plots of rate of ATP hydrolysis versus ATP concentration for (a) MopR^{A+C} and (b) MopR^{C}. Also shown are the Hill coefficients at different protein concentrations for (c) MopR^{A+C} and (d) MopR^{C}.

and 15 ± 4 μM^{-2}, respectively. In the case of MopR^{C}, respective values of 0.55 ± 0.05 s^{-1} and 0.09 ± 0.07 μM^{-5} were obtained. The linearity in the curves (Fig. 2) beyond a certain protein concentration, which is observed for both constructs, indicates that at these concentrations only an active hexameric species is present. Additionally, it was observed that complete hexamerization of MopR^{A+C} is favored at a much lower monomeric protein concentration than MopR^{C}, thereby indicating the importance of the signal reception domain in hexamer assembly. The free energy change calculated from K_{eq} for the hexamer transition of MopR^{A+C} at 25°C is −6.6 ± 0.3 $kJmol^{-1}$ and, thus, marginally more favorable than that of MopR^{C}, which is 5.9 ± 0.7 $kJmol^{-1}$. The Walker A mutant (K279A), which is unable to effectively bind ATP (12), and the Walker B mutant (E345A), which is known to not hydrolyze ATP (12), were also generated to eliminate the possibility that the measured ATP hydrolysis is due to background ATPase contamination. The purified mutants were more than 95% pure (Fig. S1) and, as expected, show no ATPase activity, thereby confirming that the observed ATPase activity in Fig. 2 is solely due to the MopR protein.

Given the protein concentration dependence of MopR's ATPase activity (Fig. 2), we measured the rate of ATP hydrolysis for both both MopR^{A+C} and MopR^{C}, as a function of ATP concentration, at protein concentrations where only the active hexameric

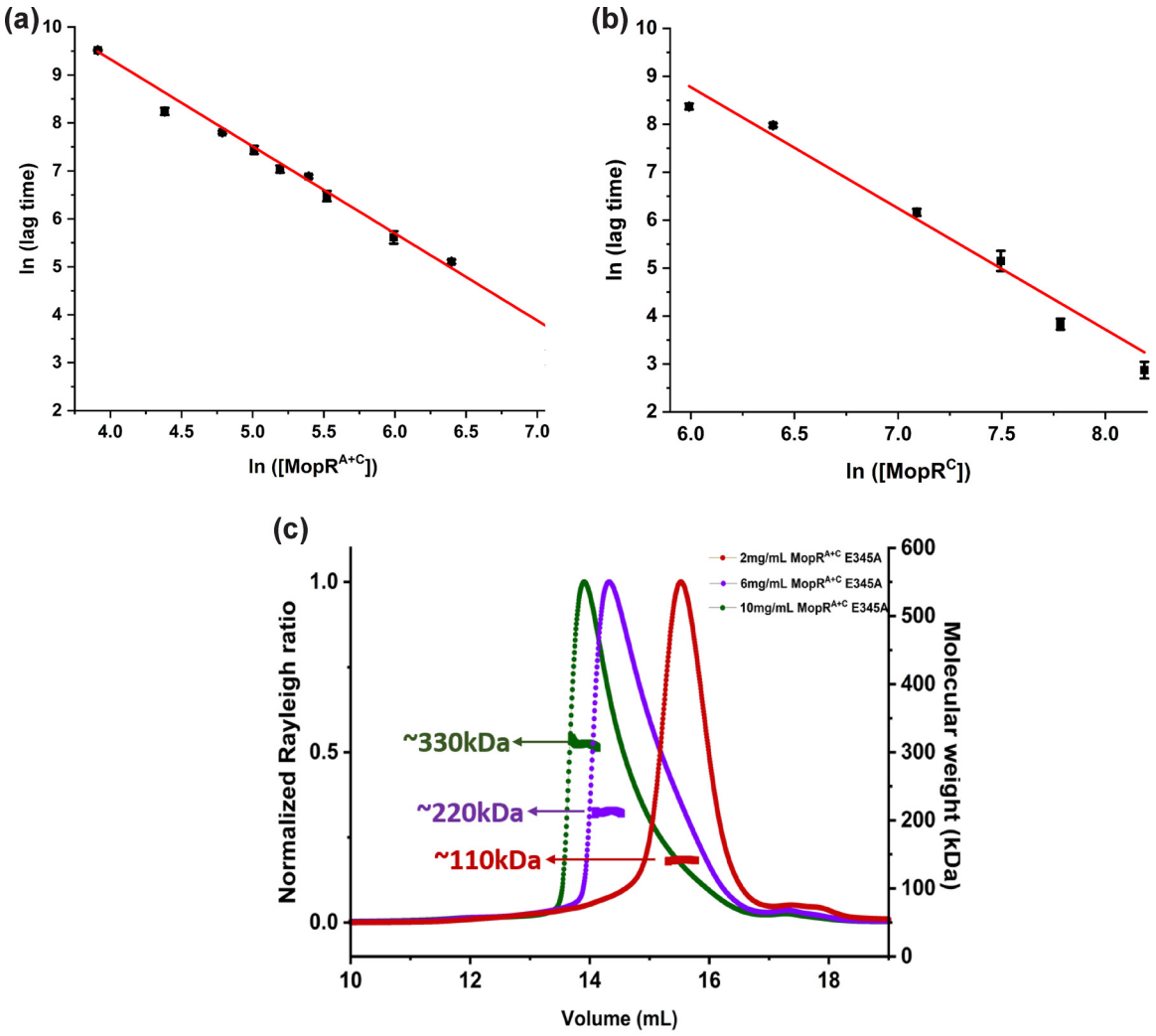

FIG 4 Assembly kinetics. Double-logarithmic plots of lag time versus concentrations of (a) MopR^{A+C} and (b) MopR^{C}. (c) SEC-MALS profile of MopR^{A+C} E345A mutant in the presence of ATP.

species is present (0.6 to 1.2 μM for MopR^{A+C} and 2.6–3.1 μM for MopR^{C}) (Fig. 3a and b). The curves were found to be sigmoidal, thereby indicating cooperativity in ATP binding and hydrolysis, with respect to ATP, and the data were fitted to the Hill equation (Equation 6). The values of the Hill coefficients for MopR^{A+C} and MopR^{C} were found to be ~1.8 and ~4.0, respectively, indicating the existence of positive cooperativity (Fig. 3c and d). The values of the Hill coefficients for both MopR^{A+C} and MopR^{C} are independent of protein concentration, thereby indicating no role of protein concentration (at this concentration range) in the conformational allostery (Fig. 3c and d). The average k_{cat} values for all the protein concentrations measured here are 0.09 $\pm$ 0.006 s^{-1} for MopR^{A+C} and 0.56 $\pm$ 0.02 s^{-1} for MopR^{C}, further confirming that there exist only a hexameric species at the various protein concentrations employed here. Reassuringly, these values of k_{cat} are in excellent agreement with those determined by an independent approach (Fig. 2). According to the concerted Monod-Wyman-Changeux model of allostery (10), such cooperativity (Fig. 3a to d) can arise when the protein is in equilibrium between two conformational states with low (T state) and high (R state) affinities for the substrate (ATP).

The progress curves of the ATPase activities of MopR^{A+C} and MopR^{C}, in the presence of a saturating concentration of ATP (7 mM), were found to display an initial lag phase that is protein concentration dependent. Such a lag phase can indicate nucleation-dependent

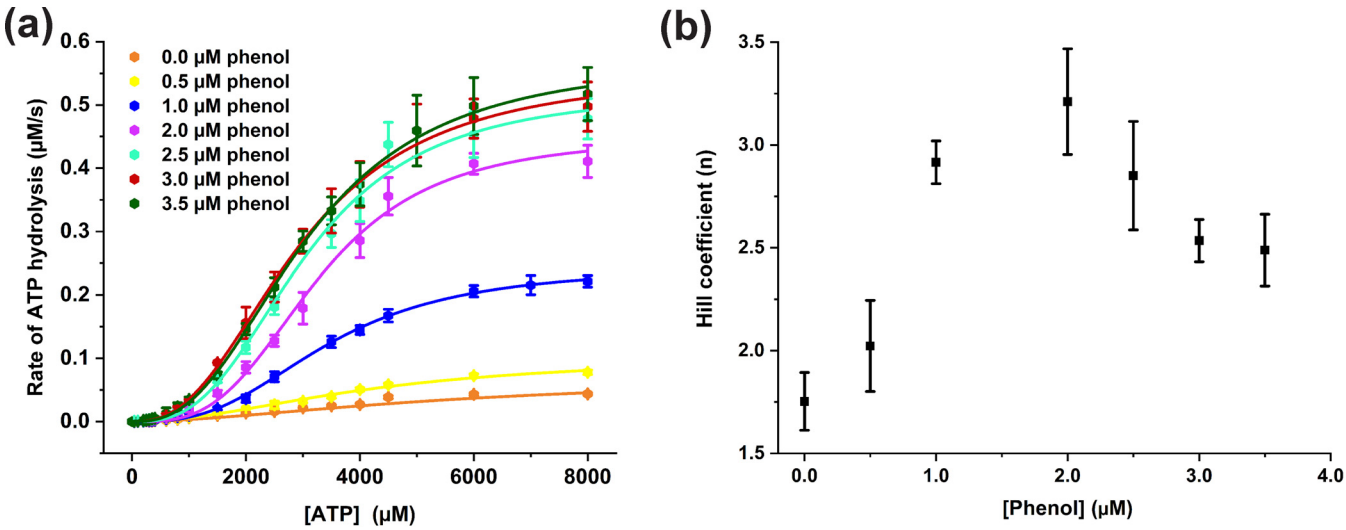

FIG 5 Effect of phenol concentration. (a) Plots of the rate of ATP hydrolysis versus ATP concentration for $MopR^{A+C}$ at different concentrations of phenol. (b) Values of the Hill coefficient (n) at different phenol concentrations.

oligomerization. Hence, a double-logarithmic plot was generated for the dependence of the lag phase length on the protein concentration (Fig. 4a and b).

A linear dependence was found with a slope that can be used to determine the critical number of protomers (M) in the initial nucleus formed before assembly of the final oligomeric species. The size of the nucleus was found to be 4 for $MopR^{A+C}$ and 5 for $MopR^{C}$. The presence of a tetrameric intermediate in the case of $MopR^{A+C}$ is consistent with the recently obtained crystal structure of phenol-bound DmpR (23). Since the structure was solved in the absence of ATP, but in the presence of phenol, we believe that the crystal structure of DmpR can represent this intermediate tetrameric state which is achieved before the complete active hexameric assembly is formed. The existence of concentration-dependent oligomerization from a dimer to hexamer via a tetrameric intermediate was further confirmed with SEC-MALS of $MopR^{A+C}$ and its Walker B mutant (E345A) (Fig. 4c, S2, S3). The data clearly reveal the impact of concentration on oligomerization of $MopR^{A+C}$. The fits for both tetrameric and hexameric oligomeric states from SEC-MALS were found to be better for the E345A mutant than for wild-type MopR. Since the Walker B mutant can only bind ATP but not hydrolyze it, we propose that ATP plays an ancillary role in stabilizing the higher-order assembly. In the case of the $MopR^{C}$ construct, which lacks the signal reception domain, the kinetic study indicates existence of a pentameric intermediate before the formation of a hexamer, suggesting that the orientation of the sensor domain may play a role in oligomerization. These comparisons between $MopR^{A+C}$ and $MopR^{C}$ confirm the higher tendency to assemble in the case of $MopR^{A+C}$ and the biological and evolutionary significance and the fine control exerted by the signal reception domain in this multidomain protein.

All of the above-mentioned studies were carried out in the absence of phenol. However, given that phenol serves as an inducer for MopR protein activity, we also examined the effects of phenol on the activity of $MopR^{A+C}$. To explore the role of phenol in the allosteric regulation of MopR, 0.8 μM $MopR^{A+C}$ was incubated with different concentrations of phenol (0.0–3.5 μM) and ATPase activity measurements were carried out (Fig. 5a). It can be seen that V_{max} increases as a function of phenol concentration, which could be correlated with the increased transcriptional activation as a function of phenol concentration at the cellular level. The values of the Hill coefficient are always found here to be greater than 1, suggesting the retainment of positive cooperativity even in the presence of phenol. However, to our surprise, the plot of the Hill coefficient values as a function of phenol concentration is bell-shaped with an initial rise followed by a drop in the extent of cooperativity (Fig. 5b). This profile shows that the equilibrium between the T and the R states, with respect to ATP, is affected by phenol binding most

likely because of the differential affinity of phenol for the two conformational states. The data suggest that cooperativity owing to the ATP-promoted T to R transition initially increases because phenol stabilizes the T state. However, beyond 2 μM phenol, cooperativity decreases because the T to R transition becomes blocked and the observed ATPase activity becomes progressively due to the T state. Furthermore, these data also indicate that the R state, though being the higher affinity state with respect to ATP, is the repressed state of the protein. The inducer, phenol, therefore, converts the protein from the repressed to the derepressed T state. The T state, which has a low affinity towards ATP, might be favoring the subsequent hydrolysis and release of ATP for the initiation of σ54-dependent transcription activation. As a control, the effect of phenol on the ATPase activity of MopR^C construct was also tested by incubating 2.6 μM MopR^C with different concentrations of phenol. From the values of V_{max} and n for MopR^C (Fig. S4) it can be asserted that in the absence of the sensor domain the ATPase activity is completely phenol independent.

DISCUSSION

NtrC proteins are enzymes with a modular architecture (13, 14). The ATPase activity of the central AAA+ domain is regulated by an upstream regulatory domain and the downstream mechanoenzyme function is likely facilitated via oligomerization of the central ATP hydrolyzing unit as well as via the interactions with its interacting counterparts (protein/DNA) (12, 22). Our results for MopR show that protein concentration is a critical parameter for oligomerization but that ATP might also assist in stabilizing the oligomeric state, as the lag phase was observed to be a function of ATP concentration. Moreover, it was also observed that oligomerization was possible even in the absence of phenol, thus indicating that it is not a prerequisite for this process.

To understand whether AAA+ proteins have some commonality in their mechanisms of ATPase activity and mode of oligomerization, phylogenetic classification of the AAA+ members was performed as proposed by Aravind and coworkers by exploiting the unique topological feature present in each family to differentiate between clades (Fig. 6) (8, 25). The AAA+ proteins were classified into seven clades based on the insertions in the secondary structural elements at defined places either within or adjacent to the core AAA+ fold (Fig. 6). Structural and functional analysis revealed that these insertions play a vital role in oligomerization and/or function. For instance, the clamp loader clade, which has no additional insertions, has always been reported to form stable pentamers (8, 26), whereas the initiator clade members (which include proteins such as DnaA, Orc1, etc.) harbor an insertion in their α2 that is believed to prevent them from forming closed oligomeric rings and instead promotes assembly as helical wraps (27, 28). In contrast, it appears that insertion of a β-hairpin structure at two locations, one right before the sensor I region (presensor I) and the other at the location of α2 (H2), does not disrupt the closed assembly but rather promotes functional interactions (Fig. 6). The crystal structure of the AAA+ domain of the PspF protein from the NtrC family (H2 insert clade) shows that these insertions protrude out of the central pore and likely participate in interaction with both the DNA and partner proteins (29). Further, the high-resolution cryo-EM structure of the AAA+ PspF protein in complex with a DNA σ54-RNA polymerase complex confirms that indeed H2 acts as a tweezer that juts out of the central pore and clasps σ54 (29). A mutation in this H2 insertion eliminates the downstream σ54-RNA polymerase-mediated transcription activity, highlighting that proper placement of these loops is paramount for function (12). In the HCLR clade, the presensor I hairpin has also been shown to be necessary for interacting with the DNA (30). In the case of the clade superfamily III, the helicase interacts with its partner protein (31) via these appendages, and the downstream function has been shown to be hampered by disrupting these interactions. A study of dynein, a member of the PSII insert clade, which has both the presensor I and H2 insertion and is evolutionarily most similar to the NtrC clade, also shows that alteration in these central pore insertions can have impairing effects on the interdomain interaction

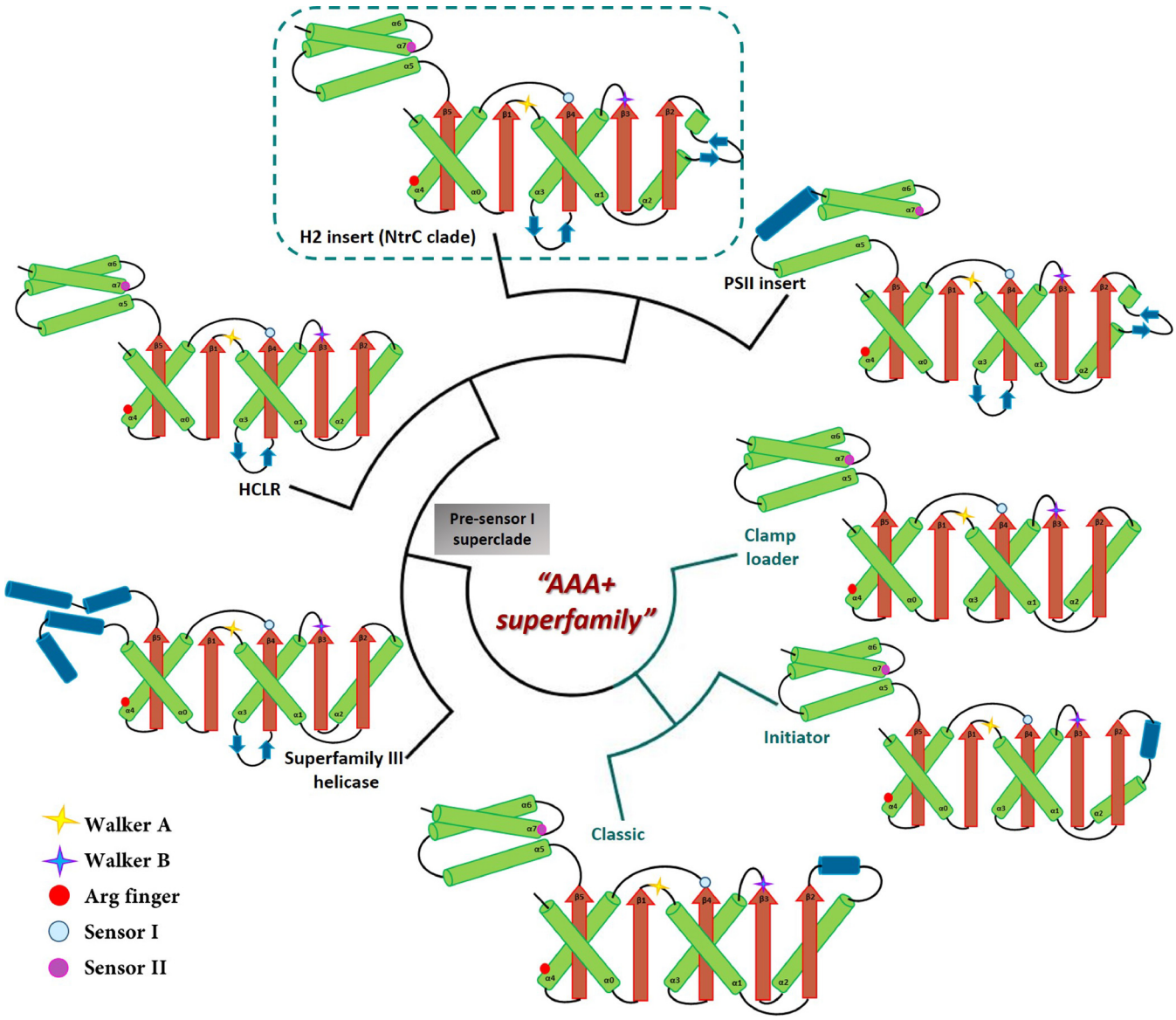

FIG 6 Schematic representation of various clades of the AAA+ superfamily highlighting their secondary structure characteristics in the form of the topology diagram. The basic secondary structures are represented in green (α-helix) and orange (β-sheets). The unique structural insertions are shown in navy blue.

and ATP hydrolysis (32). Thus, we believe an adequately assembled closed state AAA+ structure is a prerequisite for the proper orientation of these β-hairpins. Moreover, another important common feature observed in these clades is that proteins that possess these β-hairpin insertions also exhibit concentration-dependent oligomerization and assembly transitions via an intermediate state. For instance, LonA from the HCLR clade has been shown to transition from a dimer to a hexamer via a tetrameric intermediate (33). Similarly, ClpA has also been shown to form a hexamer via a tetrameric intermediate (34). We report a similar scenario in the case of MopR where the assembly progresses from a dimeric to a hexameric form via a tetrameric intermediate in a protein concentration-dependent manner. The recently solved structure of DmpR, which is a close homolog of MopR, is consistent with our biochemical observations. DmpR was solved in the phenol-bound state as a tetramer where the organization is head to tail with the signal reception domain being in closer proximity to the adjacent AAA+ unit (23). In this state, however, the β-hairpin insertions extend out and are unlikely to interact with the σ54-RNA polymerase and DNA. We, therefore, believe that the

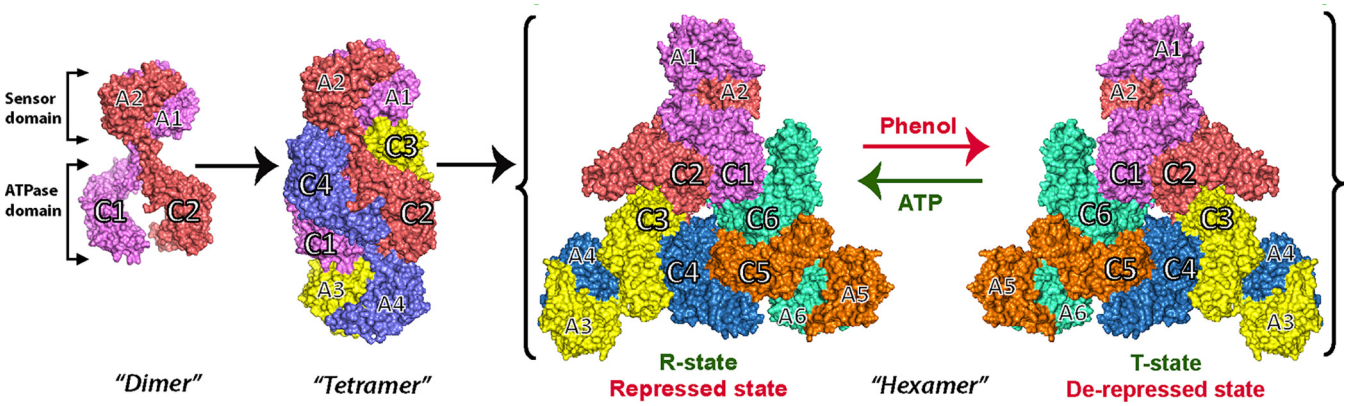

FIG 7 Model of allostery. MopR^{A+C} undergoes a transformation from dimer to hexamer via a tetrameric intermediate. The dimeric and tetrameric assemblies were generated by homology modelling using the structures of the sensor domain of MopR (PDB ID: 5KBE) and DmpR comprising both the sensor and the AAA+ ATPase domains (PDB ID: 6IY8). The hexameric ring assembly structure was generated by superimposing the homology modelled dimeric assembly of MopR^{A+C} on the AAA+ ATPase domain of PspF (PDB ID: 6NSS). Each protomer is numbered and shown in a different colour and A and C designate its sensor and AAA+ ATPase domains, respectively.

tetrameric state is an intermediate state and not a functionally active form. Based on the AAA+ superfamily literature as well as the structures and biochemical studies performed on other NtrC family proteins, we believe that the formation of the central pore, such that the β-hairpin insertions extend out of the pore grasping the key interacting elements, is a prerequisite for effecting the mechano-function of the enzyme. The biochemical data for the MopR system highlights that the hexameric assembly is the optimal oligomerization state for function.

The ATP binding sites in AAA+ proteins are generally at the dimeric interface where ATP is stabilized between the protomers via the conserved sensor I, sensor II, Walker A, and Walker B motifs along with the arginine finger motifs (7). NtrC family proteins also contain all these elements, and while the other conserved elements all reside on one protomer the arginine finger in these proteins always resides in the adjacent subunit (7). Sequential, probabilistic, and concerted models have been proposed to account for allosteric regulation of ATPase activity in various systems (35). For NtrC proteins, due to their modular architecture where the AAA+ domain is sandwiched between the upstream signal reception domains and a downstream DNA binding domain, multiple layers of controls on AAA+ activation status exist, thereby further complicating the development of a reliable allosteric model (36). In NtrC family proteins, the role of the signal reception domain has been better studied, and it has been documented that the signal reception domain can exhibit a varied effect that differs from protein to protein (12). For instance, in some members such as NtrC1, the signal reception domain has been shown to negatively regulate ATPase activity (17), whereas in the parent NtrC protein, the regulation is positive (18), i.e., no ATP hydrolysis/oligomerization is observed in the absence of the signal reception domain. However, an intermediate scenario (19) is observed in the case of NtrC4 where there is some basal activity, in the absence of the sensor molecule/modification, which is stimulated several fold upon ligand activation. MopR resembles the NtrC4 system where the presence of the signal reception domain results in negative regulation that is released upon addition of phenol.

Here, based on the kinetic data obtained in this study, we propose a basic model of allosteric regulation (Fig. 7) in which the enzyme undergoes protein concentration-dependent oligomerization from dimer to hexamer via a tetrameric intermediate. This hexameric assembly subsequently shuttles between a tense (T) state that has a lower affinity for ATP and a relaxed (R) state with a higher affinity for ATP. The equilibrium between the two states is further regulated by phenol concentration. Our experiments show that phenol stabilizes the T state and thus prompts ATP hydrolysis. However, at higher phenol concentrations due to the predominance of the T state, cooperativity decreases. This model describes the overall effect of phenol on the entire AAA+ hexameric unit and implies that the internal

rearrangement of the individual protomers in the AAA+ assembly may have a direct bearing on the phenol sensing domain conformation.

In summary, we have been able to identify several key elements in the allosteric regulation of MopR. In particular, we have shown that MopR exists in an equilibrium between different oligomeric states and undergoes a concentration-dependent transition from a lower oligomeric state to a higher oligomeric state. Additionally, this study shows that the protein's signal reception domain affects the oligomerization profile of the protein, since we observed a dimer-hexamer equilibrium in the case of $MopR^{A+C}$ but a monomer-hexamer equilibrium in the case of $MopR^{C}$. The oligomerization appears to take place via a tetrameric intermediate in the case of $MopR^{A+C}$ and a pentameric one in the case of $MopR^{C}$. Furthermore, we have also demonstrated the significance of phenol in derepressing the protein that becomes more primed for subsequent transcription activation. The knowledge obtained here may contribute to understanding the functioning of other NtrC superfamily members.

MATERIALS AND METHODS

Molecular biology and protein expression. The $MopR^{A+C}$ (that encodes residues 1 to 500) and $MopR^{C}$ (that encodes residues 205 to 500) genes were cloned from genomic DNA of *Acinetobacter calcoaceticus* NCIB8250 into a modified pET28a expression vector (Fig. 1b and c) (20). The Walker A (K279A) and Walker B (E345A) point mutants were generated by site-directed mutagenesis protocol using the Phusion DNA polymerase from New England Biolabs. The products obtained were confirmed on 0.8% agarose gel. The products were then digested with DpnI for 2 h at 37°C and transformed into *E.coli* DH5α cells. The single colonies obtained were processed for plasmid isolation. All the mutations in the obtained clones were confirmed by DNA sequencing. *Escherichia coli* BL2(DE3) pLysS cells transformed with these constructs were grown at 37°C until an OD_{600} of 0.6 to 0.8 was reached and protein expression was then induced by adding 0.7 mM IPTG (isopropyl-β-D-thiogalactopyranoside). The cells were then grown at 16°C for 16 h and harvested by centrifugation at 4000 rpm for 20 min. Both $MopR^{A+C}$ and $MopR^{C}$ (Fig. 1b and c) proteins were expressed as C-terminal His-tag fusion proteins.

Protein purification. The harvested cells were resuspended in lysis buffer (50 mM HEPES buffer [pH 7.5] containing 2 mM imidazole and 200 mM NaCl), lysed, and centrifuged. The supernatant was applied to a His-Trap HP column (GE Healthcare). The column was then washed with 50 mM HEPES buffer (pH 7.5) containing 30 mM imidazole and 200 mM NaCl. The protein was then eluted with a linear gradient of imidazole (50 to 500 mM) in 50 mM HEPES buffer (pH 7.5) containing 20 mM NaCl. The eluted protein was further purified by gel filtration in 25 mM HEPES buffer (pH 7.5) containing 100 mM NaCl and 0.5 mM DTT using a GE Healthcare Superose 6 10/300 GL column. The purity of proteins was tested by running proteins on 15% SDS-PAGE gel followed by Coomassie staining (Fig. S1). The protein-containing fractions were pooled, concentrated, flash-frozen in liquid N_2, and stored at −80°C until use.

ATPase assays. The ATPase activities of $MopR^{A+C}$ and $MopR^{C}$ were determined by monitoring the change in fluorescence intensity as a function of time of MDCC (7-diethylamino-3-((((2-maleimidyl)ethyl) amino)carbonyl)coumarin)-labeled PBP (phosphate-binding protein). PBP was expressed, purified, and labeled as described before (37). ATP hydrolysis reactions were initiated by mixing equal volumes of $MopR^{A+C}$ or $MopR^{C}$ and 16 μM PBP-MDCC with known concentrations of ATP. In the case of measurements in the presence of phenol, fixed concentrations of phenol were incubated with protein samples for 10 min prior to mixing with ATP. The reaction progress was monitored by exciting at 430 nm and measuring the fluorescence emission at 475 nm using a Fluorolog-3 fluorimeter (Horiba Jobin Yvon, Edison, NJ). All the reactions were carried out at 25°C in 25 mM HEPES buffer (pH 7.5) containing 100 mM NaCl, 10 mM $MgCl_2$ and 0.5 mM DTT.

Data analysis. The rate of ATP hydrolysis was determined using a calibration curve for MDCC-PBP with known concentrations of phosphate. All data fitting was carried out in Origin 2019b. The effect of protein concentration on the ATPase activity was determined in order to ascertain whether the protein is in equilibrium between different oligomeric states. We assumed that the active hexameric form of the protein, E_6, is in equilibrium with an inactive monomeric or dimeric form with an equilibrium constant:

$$K = [E_6]/[E_N]^m \quad (1)$$

where m = 6 for N = 1 and m = 3 for N = 2. The maximum initial rate of ATP hydrolysis (V_{max}) at saturating substrate (ATP) concentration, is given by

$$V_{max} = k_{cat}[E_6] \quad (2)$$

where k_{cat} is the catalytic rate constant of E_6. Combining equations (1) and (2) yields

$$V_{max} = k_{cat} K [E_N]^m \quad (3)$$

The total enzyme monomer concentration ($[E_t]$) is

$$[E_t] = 6[E_6] + N[E_N] \quad (4)$$

Combining equations (2)-(4) leads to the following equation for fitting the data:

$$[E_t] = \alpha V_{max} + \beta V_{max}^{1/m} \quad (5)$$

where m = 6 for N = 1 or m = 3 for N = 2, $\alpha = 6/k_{cat}$ and $\beta = N(1/k_{cat}\,K)^{1/m}$. The data in Fig. 2 were fitted to equation (5) for m = 6 or m = 3.

(i) Analysis of cooperativity. Plots of initial rates of ATP hydrolysis as a function of ATP concentration were used for analysis of cooperativity. The data (Fig. 3a, b and Fig. 5a) were fitted to the Hill equation (38),

$$V = K[S]^n/(1 + K[S]^n) \quad (6)$$

where V is the initial velocity, [S] is the ATP concentration, K is the apparent binding constant and n is the Hill coefficient.

(ii) Assembly kinetics. A lag phase is observed when ATP hydrolysis by MopR is monitored by measuring the change in fluorescence intensity of PBP-MDCC as a function of time. The lag phase can be an indication of nucleation-dependent polymerization (39, 40). Such measurements were carried out with various concentrations of protein at a fixed, saturating concentration of ATP. It has been proposed that the length of the lag phase scales inversely to [monomer]$^{M/2}$ where M is the number of monomers involved in the critical step for initial assembly. Plots of ln(lag time) versus ln ([monomer]) (Fig. 4) were generated to obtain the value of M.

Size exclusion chromatography coupled to multi-angle light scattering (SEC-MALS) study. SEC−MALS was performed at different concentrations of native MopR^{A+C} and its Walker B mutant (E345A) in the presence of ATP. The samples were loaded on a Superose 6 10/300 analytical gel filtration column (GE Healthcare) running at 0.4 mL/min, connected to an Agilent HPLC system in tandem with the 18-angle light scattering detector (Wyatt Dawn HELIOS II) and a refractive index detector (Wyatt Optilab TrEX). Prior to the experiment, the system was equilibrated with the ATPase assay buffer and subsequent calibration was carried out with BSA at a concentration of 2 mg/mL; the molecular weights were calculated using ASTRA software (Wyatt Technologies).

SUPPLEMENTAL MATERIAL

Supplemental material is available online only.

SUPPLEMENTAL FILE 1, PDF file, 0.5 MB.

ACKNOWLEDGMENTS

The work of J.S. at the Weizmann Institute of Science was supported by an EMBO short-term fellowship (STF number: 8301). R.A. acknowledges support of DST, Government of India (Project No. DST/TMD/EWO/WTI/2K19/EWFH/2019/48). J.S. thanks Ilia Korobko for his helpful advice. The authors also thank Radha Chauhan for providing access to SEC-MALS facility at National Centre for Cell Science, Pune, India.

REFERENCES

1. Vale RD. 2000. AAA proteins. Lords of the ring. J Cell Biol 150:F13–F19. https://doi.org/10.1083/jcb.150.1.f13.
2. Gates SN, Martin A. 2020. Stairway to translocation: AAA+ motor structures reveal the mechanisms of ATP-dependent substrate translocation. Protein Sci 29:407–419. https://doi.org/10.1002/pro.3743.
3. Martin A, Baker TA, Sauer RT. 2005. Rebuilt AAA + motors reveal operating principles for ATP-fuelled machines. Nature 437:1115–1120. https://doi.org/10.1038/nature04031.
4. Wendler P, Shorter J, Snead D, Plisson C, Clare DK, Lindquist S, Saibil HR. 2009. Motor mechanism for protein threading through Hsp104. Mol Cell 34:81–92. https://doi.org/10.1016/j.molcel.2009.02.026.
5. Maillard RA, Chistol G, Sen M, Righini M, Tan J, Kaiser CM, Hodges C, Martin A, Bustamante C. 2011. ClpX(P) generates mechanical force to unfold and translocate its protein substrates. Cell 145:459–469. https://doi.org/10.1016/j.cell.2011.04.010.
6. Aubin-Tam ME, Olivares AO, Sauer RT, Baker TA, Lang MJ. 2011. Single-molecule protein unfolding and translocation by an ATP-fueled proteolytic machine. Cell 145:257–267. https://doi.org/10.1016/j.cell.2011.03.036.
7. Wendler P, Ciniawsky S, Kock M, Kube S. 2012. Structure and function of the AAA+ nucleotide binding pocket. Biochim Biophys Acta 1823:2–14. https://doi.org/10.1016/j.bbamcr.2011.06.014.
8. Erzberger JP, Berger JM. 2006. Evolutionary relationships and structural mechanisms of AAA+ proteins. Annu Rev Biophys Biomol Struct 35:93–114. https://doi.org/10.1146/annurev.biophys.35.040405.101933.
9. Dougan DA, Mogk A, Zeth K, Turgay K, Bukau B. 2002. AAA+ proteins and substrate recognition, it all depends on their partner in crime. FEBS Lett 529:6–10. https://doi.org/10.1016/s0014-5793(02)03179-4.
10. Monod J, Wyman J, Changeux JP. 1965. On the nature of allosteric transitions: a plausible model. J Mol Biol 12:88–118. https://doi.org/10.1016/S0022-2836(65)80285-6.
11. Koshland DE, Jr, Nemethy G, Filmer D. 1966. Comparison of experimental binding data and theoretical models in proteins containing subunits. Biochemistry 5:365–385. https://doi.org/10.1021/bi00865a047.
12. Bush M, Dixon R. 2012. The role of bacterial enhancer binding proteins as specialized activators of σ54-dependent transcription. Microbiol Mol Biol Rev 76:497–529. https://doi.org/10.1128/MMBR.00006-12.
13. Kustu S, North AK, Weiss DS. 1991. Prokaryotic transcriptional enhancers and enhancer-binding proteins. Trends Biochem Sci 16:397–402. https://doi.org/10.1016/0968-0004(91)90163-P.
14. Morett E, Segovia L. 1993. The sigma 54 bacterial enhancer-binding protein family: mechanism of action and phylogenetic relationship of their functional domains. J Bacteriol 175:6067–6074. https://doi.org/10.1128/jb.175.19.6067-6074.1993.
15. Bordes P, Wigneshweraraj SR, Schumacher J, Zhang X, Chaney M, Buck M. 2003. The ATP hydrolyzing transcription activator phage shock protein F of *Escherichia coli*: identifying a surface that binds sigma 54. Proc Natl Acad Sci U S A 100:2278–2283. https://doi.org/10.1073/pnas.0537525100.
16. Rappas M, Schumacher J, Beuron F, Niwa H, Bordes P, Wigneshweraraj S, Keetch CA, Robinson CV, Buck M, Zhang X. 2005. Structural insights into

the activity of enhancer-binding proteins. Science 307:1972–1975. https://doi.org/10.1126/science.1105932.
17. Lee SY, De La Torre A, Yan D, Kustu S, Nixon BT, Wemmer DE. 2003. Regulation of the transcriptional activator NtrC1: structural studies of the regulatory and AAA+ ATPase domains. Genes Dev 17:2552–2563. https://doi.org/10.1101/gad.1125603.
18. Lee J, Owens JT, Hwang I, Meares C, Kustu S. 2000. Phosphorylation-induced signal propagation in the response regulator NtrC. J Bacteriol 182:5188–5195. https://doi.org/10.1128/JB.182.18.5188-5195.2000.
19. Batchelor JD, Doucleff M, Lee C-J, Matsubara K, De Carlo S, Heideker J, Lamers MH, Pelton JG, Wemmer DE. 2008. Structure and regulatory mechanism of Aquifex aeolicus NtrC4: variability and evolution in bacterial transcriptional regulation. J Mol Biol 384:1058–1075. https://doi.org/10.1016/j.jmb.2008.10.024.
20. Ray S, Gunzburg MJ, Wilce M, Panjikar S, Anand R. 2016. Structural basis of selective aromatic pollutant sensing by the effector binding domain of MopR, an NtrC family transcriptional regulator. ACS Chem Biol 11:2357–2365. https://doi.org/10.1021/acschembio.6b00020.
21. Patil VV, Park KH, Lee SG, Woo E. 2016. Structural analysis of the phenol-responsive sensory domain of the transcription activator PoxR. Structure 24:624–630. https://doi.org/10.1016/j.str.2016.03.006.
22. Schumacher J, Joly N, Rappas M, Zhang X, Buck M. 2006. Structures and organisation of AAA+ enhancer binding proteins in transcriptional activation. J Struct Biol 156:190–199. https://doi.org/10.1016/j.jsb.2006.01.006.
23. Park KH, Kim S, Lee SJ, Cho JE, Patil VV, Dumbrepatil AB, Song HN, Ahn WC, Joo C, Lee SG, Shingler V, Woo EJ. 2020. Tetrameric architecture of an active phenol-bound form of the AAA^+ transcriptional regulator DmpR. Nat Commun 11:2728. https://doi.org/10.1038/s41467-020-16562-5.
24. Fernández I, Cornaciu I, Carrica MD, Uchikawa E, Hoffmann G, Sieira R, Márquez JA, Goldbaum FA. 2017. Three-dimensional structure of full-length NtrX, an unusual member of the NtrC family of response regulators. J Mol Biol 429:1192–1212. https://doi.org/10.1016/j.jmb.2016.12.022.
25. Iyer LM, Leipe DD, Koonin EV, Aravind L. 2004. Evolutionary history and higher order classification of AAA+ ATPases. J Struct Biol 146:11–31. https://doi.org/10.1016/j.jsb.2003.10.010.
26. Gaubitz C, Liu X, Magrino J, Stone NP, Landeck J, Hedglin M, Kelch BA. 2020. Structure of the human clamp loader reveals an autoinhibited conformation of a substrate-bound AAA+ switch. Proc Natl Acad Sci U S A 117:23571–23580. https://doi.org/10.1073/pnas.2007437117.
27. Cunningham EL, Berger JM. 2005. Unraveling the early steps of prokaryotic replication. Curr Opin Struct Biol 15:68–76. https://doi.org/10.1016/j.sbi.2005.01.003.
28. Erzberger JP, Mott ML, Berger JM. 2006. Structural basis for ATP-dependent DnaA assembly and replication-origin remodeling. Nat Struct Mol Biol 13:676–683. https://doi.org/10.1038/nsmb1115.
29. Glyde R, Ye F, Darbari VC, Zhang N, Buck M, Zhang X. 2017. Structures of RNA polymerase closed and intermediate complexes reveal mechanisms of DNA opening and transcription initiation. Mol Cell 67:106–116.e4. https://doi.org/10.1016/j.molcel.2017.05.010.
30. Han YW, Iwasaki H, Miyata T, Mayanagi K, Yamada K, Morikawa K, Shinagawa H. 2001. A unique β-hairpin protruding from AAA+ ATPase domain of RuvB motor protein is involved in the interaction with RuvA DNA recognition protein for branch migration of Holliday junctions. J Biol Chem 276:35024–35028. https://doi.org/10.1074/jbc.M103611200.
31. Gai D, Zhao R, Li D, Finkielstein CV, Chen XS. 2004. Mechanisms of conformational change for a replicative hexameric helicase of SV40 large tumor antigen. Cell 119:47–60. https://doi.org/10.1016/j.cell.2004.09.017.
32. Bhabha G, Cheng HC, Zhang N, Moeller A, Liao M, Speir JA, Cheng Y, Vale RD. 2014. Allosteric communication in the dynein motor domain. Cell 159:857–868. https://doi.org/10.1016/j.cell.2014.10.018.
33. Rudyak SG, Brenowitz M, Shrader TE. 2001. Mg^{2+}-linked oligomerization modulates the catalytic activity of the Lon (La) protease from *Mycobacterium smegmatis*. Biochemistry 40:9317–9323. https://doi.org/10.1021/bi0102508.
34. Kress W, Mutschler H, Weber-Ban E. 2007. Assembly pathway of an AAA+ protein: tracking ClpA and ClpAP complex formation in real time. Biochemistry 46:6183–6193. https://doi.org/10.1021/bi602616t.
35. Kainov DE, Tuma R, Mancini EJ. 2006. Hexameric molecular motors: P4 packaging ATPase unravels the mechanism. Cell Mol Life Sci 63:1095–1105. https://doi.org/10.1007/s00018-005-5450-3.
36. Gruber R, Horovitz A. 2018. Unpicking allosteric mechanisms of homo-oligomeric proteins by determining their successive ligand binding constants. Philos Trans R Soc B 373:20170176. https://doi.org/10.1098/rstb.2017.0176.
37. Brune M, Hunter JL, Corrie JE, Webb MR. 1994. Direct, realtime measurement of rapid inorganic phosphate release using a novel fluorescent probe and its application to actomyosin subfragment 1 ATPase. Biochemistry 33:8262–8271. https://doi.org/10.1021/bi00193a013.
38. Hill AV. 1910. The possible effects of the aggregation of the molecules of haemoglobin on its dissociation curves. J Physiol 40:IV–VII.
39. Dobson CM. 2003. Protein folding and misfolding. Nature 426:884–890. https://doi.org/10.1038/nature02261.
40. Oosawa F, Asakura S. 1975. Thermodynamics of the polymerization of protein. Academic Press, London.